10.1109/ULTSYM.2010.0578

Ultrasound Speckle Reduction using Coded Excitation, Frequency Compounding, and Post-processing Despeckling Filters

Joshua S. Ullom
Department 3434, Airborne & Security SW
Harris Corporation
Palm Bay, Florida 32905
Email: joshua.s.ullom@gmail.com

Michael Oelze
ECE Department
University of Illinois at Urbana-Champaign
Urbana, Illinois 61801
Email: oelze@illinois.edu

Jose R. Sanchez
Electrical and Computer Engineering Department
Bradley University
Peoria, Illinois 61625
Email: jsm@bradley.edu

***Abstract*—A technique for improvement of ultrasonic B-mode imaging that uses coded excitation, pulse compression, and frequency compounding was developed. A coded excitation and pulse compression technique known as resolution enhancement compression (REC) was used to enhance the bandwidth of an imaging system by a factor of two. This bandwidth was subdivided into smaller subbands through the speckle-reducing technique known as frequency compounding (REC-FC). Frequency compounded images were generated using various subband widths and then averaged to reduce speckle and to improve contrast while preserving spatial resolution, known as enhanced REC-FC (eREC-FC). In this study, further improvements in contrast and reduction in speckle were obtained by applying post-processing despeckling filters. The following post-processing despeckling filters were explored and analyzed in regard to contrast improvement, speckle reduction, and image feature preservation: median, Lee, homogeneous mask area, geometric, and speckle reducing anisotropic diffusion (SRAD). To quantify the performance of each filter, contrast-to-noise ratio was used. Data from thirty simulated phantoms and experimental data from a tissue-mimicking phantom were generated and filtered. Results demonstrated that post-processing despeckling filters coupled with the eREC-FC technique could improve the image by up to 563%, in terms of the contrast-to-noise ratio, when compared to conventional ultrasonic imaging.**

Keywords- Coded excitation; contrast improvement; frequency compounding; pulse compression; speckle reduction; ultrasound

I. INTRODUCTION

Ultrasonic images are corrupted with system-dependent imperfections called speckle. Observed as granular distortions, speckle is multiplicative noise that can mask small or low-contrast lesions. Speckle can be a problem in diagnostic ultrasound, especially in the area of early detection of cancerous lesions. These lesions are often either low-contrast or so small that the effects of speckle make the lesion imperceptible. It is desired to detect tumors as early as possible, and the effects of speckle may inhibit early detection.

The overall quality of ultrasound (US) images can be improved through averaging methods or post-processing. Examples of averaging methods include the use of frequency compounding [1-2] and spatial compounding [3-4].

A novel averaging scheme was recently developed. This process starts with resolution enhancement compression (REC), which uses a pre-enhanced chirp to double the resolution of the image [5]. By using a pre-enhanced chirp to excite the US transducer instead of conventional pulsing (CP), the effective impulse response can be forced into a more desirable response. The pre-enhanced chirp was obtained through convolution equivalence to force the effective impulse response of the imaging system to have twice the bandwidth of the natural impulse response of the system. Thus, the increase in resolution of REC translates directly to an increase in the bandwidth of the image.

REC was implemented along with frequency compounding (REC-FC) to improve contrast and reduce speckle [6]. In FC, the spectra of the radio frequency (RF) echo data were subdivided using subband filters to generate partially uncorrelated speckle images. By compounding the resulting images, speckle was reduced in the resulting image. Because of the larger bandwidth of REC, more subbands could be used, allowing for more decorrelation of speckle than FC applied to CP techniques. Therefore, the tradeoff in REC-FC was contrast resolution vs. axial resolution.

Enhanced REC-FC (eREC-FC) is the compounding of several REC-FC images obtained at different subband widths [7]. There are three defining characteristics of eREC-FC. First, the axial resolution in the resulting image is comparable to CP. Second, the contrast resolution is improved over CP by a factor of two. Finally, speckle in the image is reduced. These eREC-FC images can be further improved with the addition of speckle-reducing post-processing (SRPP) filters.

Many SRPP filters have been developed to effectively eliminate or reduce speckle in US images, including Lee [8], Kuan [9], and speckle reducing anisotropic diffusion [10]. This study focuses on improving US image quality of eREC-FC US images by applying SRPP filtering techniques.

II. Methods and Procedures

The despeckling filters used are listed in this section. Most of the following filters make use of a moving, overlapping window. This is defined as a window of size ($n \times n$), where n is an odd integer, that advances through the entire image one pixel at a time. The center pixel of the window is the location that will be adjusted in the filtered image. In eREC-FC iterative techniques, after the first iteration (filtering of the original image), the filtered image becomes the input to the filter for each successive iteration.

A. Filter Descriptions

Median Filtering [11]: Median filtering makes use of a moving, overlapping window. The median of the pixels in the window is the resulting value of the center pixel in the window for the filtered image. Median filtering is used to smooth an image and minimize or eliminate noise spikes, with the idea that all pixels in a small region of an image should be similar.

Lee Filtering [8]: Lee filtering also uses a moving, overlapping window. The filter uses statistics within that window such as mean and variance to adjust the resulting center pixel of the window. Because the variance in noise, or speckle, is not known, it is estimated for the entire image. A window 10 times larger than the filtering window is used to estimate the speckle. Statistics on each region are combined over the entire image to obtain one estimate of noise.

Homogeneous Mask Area Filtering [12]: Two windows are used in homogeneous mask area filtering – a large main window, which determines the pixel location to filter, and a moving smaller subwindow within the main window. For each subwindow, a speckle index is calculated using the mean and variance of the pixel intensities contained in the window. The mean of region with the smallest speckle index (mean of pixel intensities divided by the variance) becomes the filtered pixel value. For this study, the subwindow size was ($n-2 \times n-2$).

Geometric Filtering [13]: Using a moving, overlapping window of size (3×3), the geometric filter uses an iterative approach to make the center pixel of the window more like its neighboring pixels. The idea behind the geometric filter is that a very small region of an image should be homogeneous. There are four directions the geometric filter iterates through – up-down, left-right, and both diagonals in a (3×3) pixel region. In each case, a line of three pixels is created for evaluation of the neighboring pixels.

Speckle Reducing Anisotropic Diffusion (SRAD) [10]*:* SRAD is an algorithm that smears the pixel intensities within homogenous regions while preserving edges by not smearing across inhomogeneous regions. SRAD is based on anisotropic diffusion and is executed by solving the diffusion equation described as a nonlinear partial differential equation, making use of the divergence and gradient of the image.

B. Image Quality Metric

Contrast-to-Noise Ratio (CNR) quantifies the degree to which one region of an image is visible in comparison to another region. For this study, a region in the lesion is compared to a region in the background. CNR is calculated as the difference between the mean of the pixel intensities divided by the square root of the summed variance of the pixel intensities of each region [14]. Because of attenuation, the CNR was calculated at the same depth for both regions. A larger CNR represents better contrast.

C. Ultrasonic Phantoms and Sources

Computer simulations were performed in MATLAB (MathWorks, Natick, MA) to generate all US images. The simulations used the received pulse-echo pressure field model observed in [15] and were made to match experimental measurements. A 2.25 MHz single-element transducer (f/2.66) with a fractional bandwidth of 50% at -3 dB was the model for

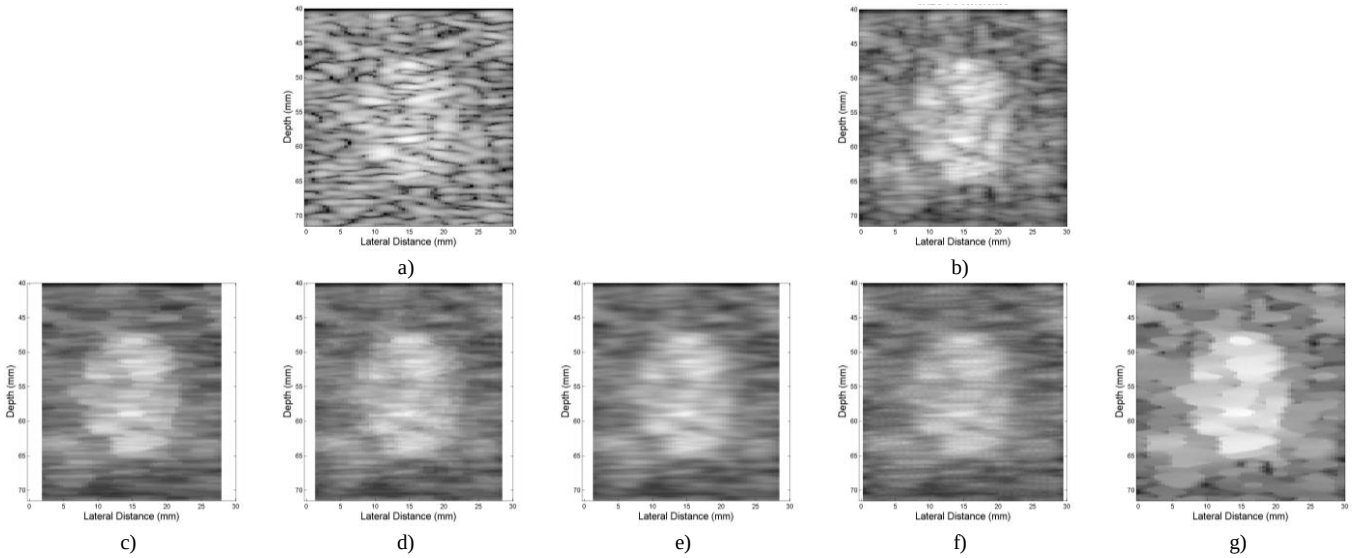

Fig.1. Reference B-mode images from one of the 30 simulated phantoms for a) CP and b) eREC-FC. B-mode images from one of the 30 simulated phantoms after applying a post-processing filter: c) median filter (9×9), d) homogeneous mask area filter (7×7), e) Lee filter (7×7), f) geometric filter (5), g) SRAD (3300). Parentheses denote ($n \times n$) window or n iterations.

TABLE I. CNR ± ONE STANDARD DEVIATION AS A FUNCTION OF FILTERING TECHNIQUE OVER THE SPAN OF WINDOW SIZES OR ITERATIONS OF 30 SIMULATED PHANTOMS

	CP	eREC-FC	Med			HMA			Lee			Geo			SRAD		
	Reference	Reference	3	7	11	5	7	11	3	7	11	1	5	9	900	2100	3300
CNR	0.8 ±0.2	2.0 ±0.3	2.9 ±0.4	3.5 ±0.5	3.9 ±0.5	3.2 ±0.4	3.6 ±0.5	4.0 ±0.5	2.9 ±0.4	3.6 ±0.5	4.1 ±0.6	3.0 ±0.4	3.6 ±0.5	3.3 ±0.5	3.8 ±0.5	4.7 ±0.6	5.3 ±0.8

CP. For REC, the impulse response of the transducer was constructed to have double the fractional bandwidth (100%) at -3 dB.

In simulations, 30 tissue-mimicking phantoms of hyperechoic (+6-dB) targets were imaged, each having 20 uniformly distributed point scatterers per resolution cell volume, in order to ensure fully developed speckle. In experimental measurements, a hyperechoic (+6-dB) target from an ATS 539 tissue-mimicking phantom was imaged. Both simulated and experimental phantoms had a target with a diameter of 12 mm.

III. RESULTS AND DISCUSSION

A. Simulation Results

The 30 simulated phantoms were filtered by applying the speckle-reducing post-processing techniques discussed in Section II-A using MATLAB. All SRPP filters were applied to images generated with a conventional pulse (CP) and coded excitation (eREC-FC). The window-based filters were all applied with window sizes of n = 3, 5, 7, 9, and 11. The geometric filter was applied in iterations of 1 through 9. SRAD was applied in iterations of $300n$, for n defined above.

All filters showed qualitative blurring across the object edges throughout the entire image except SRAD. Fig. 1 shows the reference CP and eREC-FC images along with resulting eREC-FC post-processed images. The average CNR over the 30 simulations are shown in Table I.

For every filter except geometric, the largest window or number of iterations resulted in the best CNR. The CNR improvement from geometric filtering peaked at six iterations. The increase in CNR as a function of window size or iterations followed a logarithmic-like shape. Eventually, the benefit of increasing the window size or iterations will become minimal, in addition to the drawback of increased computational time. The reference images using the eREC-FC technique exhibited a 150% CNR improvement over reference images using CP. The best window size, or iteration count, for each filter produced an additional improvement of 95%, 100%, 105%, 80%, and 165% for median (11×11), homogeneous mask area (11×11), Lee (11×11), geometric (5), and SRAD (3300), respectively, over the eREC-FC reference images. Those window sizes or iteration counts for each filter provided a total CNR improvement (from CP reference image to filtered eREC-FC image) for each filter was 388%, 400%, 413%, 350%, and 563% for median, homogeneous mask area, Lee, geometric, and SRAD, respectively over the CP reference image.

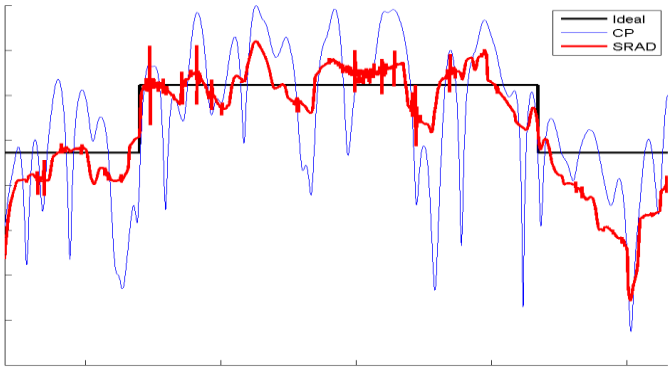

Fig. 2. Comparative axial profile of simulated data. Black, blue, and red denote ideal, conventional pulsing, and SRAD axial profiles, with depth on the abscissa and magnitude on the ordinate.

The axial profile through the center of the lesion from one of the CP and SRAD-filtered images were compared as shown in Fig. 2. In addition, the profile of the simulated lesion prior to ultrasound imaging is shown. The CP profile varies greatly around each region (lesion, background) and is difficult to properly distinguish the boundaries of the two regions. From Fig. 2 it is evident that SRAD has significantly reduced variance in the target region. However, a slight bias was introduced in the background region. This would help explain the increases in CNR achieved with SRAD.

B. Experimental Results

An image was obtained experimentally with a transducer with the specifications described in section II-C. The image was of a +6 dB lesion, having a target of 12 mm. All filters were applied to the experimental data in MATLAB. Table II shows the CNR obtained for each of the filters applied to the experimental data from the ATS phantom.

Similar to simulation results, all filters resulted in blurring across feature edges in the entire image except SRAD. The general trends of the experimental data are somewhat similar to the simulation. Fig. 3 shows the resulting images after filtering the experimental data. For the experimental data set, the CNR for the homogeneous mask area (11×11) and Lee (11×11) filters resulted in the best improvement over CP: 317% and 333%, respectively. SRAD (3300) resulted in an

TABLE II. CNR AS A FUNCTION OF FILTERING TECHNIQUE OVER THE SPAN OF WINDOW SIZES OR ITERATIONS FOR ATS DATA.

	CP	eREC-FC	Med			HMA			Lee			Geo			SRAD		
			3	7	11	5	7	11	3	7	11	1	5	9	900	2100	3300
CNR	0.6	1.6	1.7	2.0	2.3	2.1	2.3	2.5	1.8	2.3	2.6	1.8	2.1	1.8	1.7	1.8	1.9

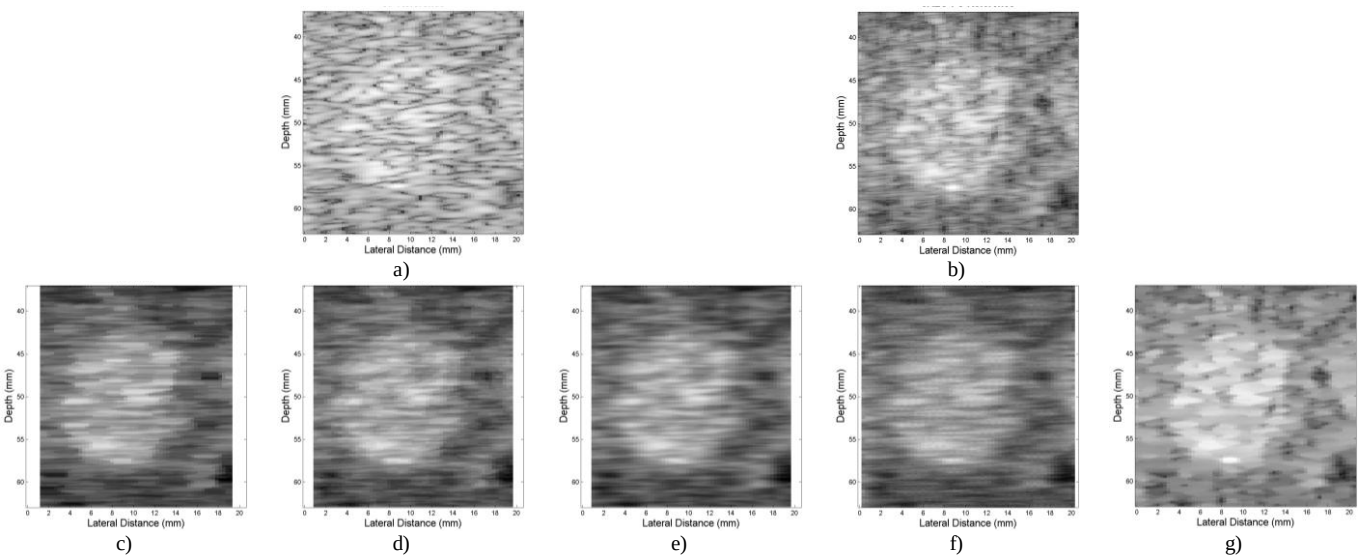

Fig. 3. Reference B-mode images from the ATS phantom experimental data for a) CP and b) eREC-FC. B-mode images obtained from experimental data after applying a post-processing filter: c) median filter (9), d) homogeneous mask area filter (7), e) Lee filter (7), f) geometric filter (5), g) SRAD (3300). Parenthesis denote (n x n) window or n iterations.

improvement of 217% CNR improvement over CP.

IV. DISCUSSION AND CONCLUSION

In this study, the quality of US images obtained through the eREC-FC technique was significantly improved through the application of post-processing despeckling filters.

SRAD has been shown to be an impressive filter on CP filtering [16]. The eREC-FC technique morphs speckle as a result of the signal processing techniques it uses. Consequently, despite significant improvements when compared to the reference images and other post-processing filters, SRAD applied to the experimental data did not result in the best CNR improvement. The altered speckle from eREC-FC could explain why other filters, such as the Lee, which is known for its noise- and speckle-reducing properties, and the homogeneous mask area filters performed the best on experimental eREC-FC reference images.

A possible extension of this work would be to evaluate how these post-processed images perform when attempting segmentation techniques. Consequently, segmented regions could be used to superimpose the edges of the object on the image with the best feature as quantified by several image quality metrics. Further work could include implementation of the eREC-FC technique with some filtering techniques in hardware and evaluation of the performance of these techniques for detecting small lesions.

REFERENCES

[1] S. M. Gehlbach and F. G. Sommer, "Frequency diversity speckle processing," *Ultrason. Imaging*, vol. 9, pp. 92-105, Apr. 1987.

[2] P. A. Magnin, O. T. von Ramm, and F. L. Thurstone, "Frequency compounding for speckle contrast reduction in phased array images," *Ultrason. Imaging*, vol. 4, pp. 267-281, Jul. 1982.

[3] S. K. Jespersen, J. E. Wilhjelm, and H. Sillensen, "Multi-angle compound imaging," *Ultrason. Imaging*, vol. 20, no. 2, pp. 81-102, Apr. 1998.

[4] A. R. Groves and R. N. Rohling, "Two-dimensional spatial compounding with warping," *Ultrasound Med. Biol.*, vol. 30, no. 7, pp. 929-942, Jul. 2004.

[5] M. L. Oelze, "Bandwidth and resolution enhancement through pulse compression," *IEEE Trans. Ultrason., Ferroelectr. Freq. Contr.*, vol. 54, no. 4, p. 770, Apr. 2007.

[6] J. R. Sanchez and M. L. Oelze, "An ultrasonic imaging speckle-suppression and contrast enhancement technique by means of frequency compounding and coded excitation," *IEEE Trans. Ultrason. Ferroelectr. Freq. Control*, vol. 56, pp. 1327-1339, Jul. 2009.

[7] J. R. Sanchez, M. Orescanin, and M. Oelze, "Improving Image Contrast Using Coded Excitation for Ultrasonic Imaging," *Proceedings of the IEEE International Conference on Electro/Information Technology*, pp. 325-330, 2010.

[8] J. S. Lee, "Digital image enhancement and noise filtering by using local statistics," *IEEE Trans. Pattern Anal. Machine Intell.*, vol. PAM1-2, 1980.

[9] D. T. Kuan, A. A. Sawchuk, T. C. Strand, and P. Chavel, "Adaptive restoration of images with speckle," *IEEE Trans. Acoust., Speech, Signal Processing*, vol. ASSP-35, pp. 373–383, 1987.

[10] Y. Yu and S. T. Acton, "Speckle reducing anisotropic diffusion," *IEEE Trans. Image Process.*, vol. 11, no. 11, pp. 1260-1270, Nov. 2002.

[11] M. O. Ahmad and D. Sundararajan, "A fast algorithm for two-dimensional median filtering," *IEEE Trans. Circuits and Syst.*, vol. CAS-34, no. 11, pp. 1364-1374, Nov. 1987.

[12] C. P. Loizou, C. Christodoulou, C. S. Pattichis, R. Istepanian, M. Pantziaris, and A. Nicolaides. "Speckle reduction in ultrasound images of atherosclerotic carotid plaque," *14th International Conference on Digital Signal Processing, 2002*, vol. 2, pp. 525-528, 2002.

[13] L. J. Busse, T. R. Crimmins, and J. R. Fienup, "A model based approach to improve the performance of the geometric filtering speckle reduction algorithm," *IEEE Ultrason. Symposium*, pp. 1353-1356, 1995.

[14] M. S. Patterson and F. S. Foster, "The improvement and quantitative assessment for B-Mode images produced by an annular array / cone hybrid," *Ultrason. Imag.*, vol. 5, no. 3, pp. 195-213, Jul. 1983.

[15] J. A. Jensen, "A model for the propagation and scattering of ultrasound tissue," *J. Acoust. Soc. Am.*, vol. 89, pp. 182-190, Jan. 1991.

[16] C. P. Loizou, C. S. Pattichis, C. I. Christodoulou, R. S. H. Istepanian, M. Pantziaris, and A. Nicolaides, "Comparative evaluation of despeckle filtering in ultrasound imaging of the carotid artery," *IEEE Trans. Ultrason., Ferroelectr. Freq. Contr.*, vol. 52, no. 10, p. 1653-1669, Oct. 2005.